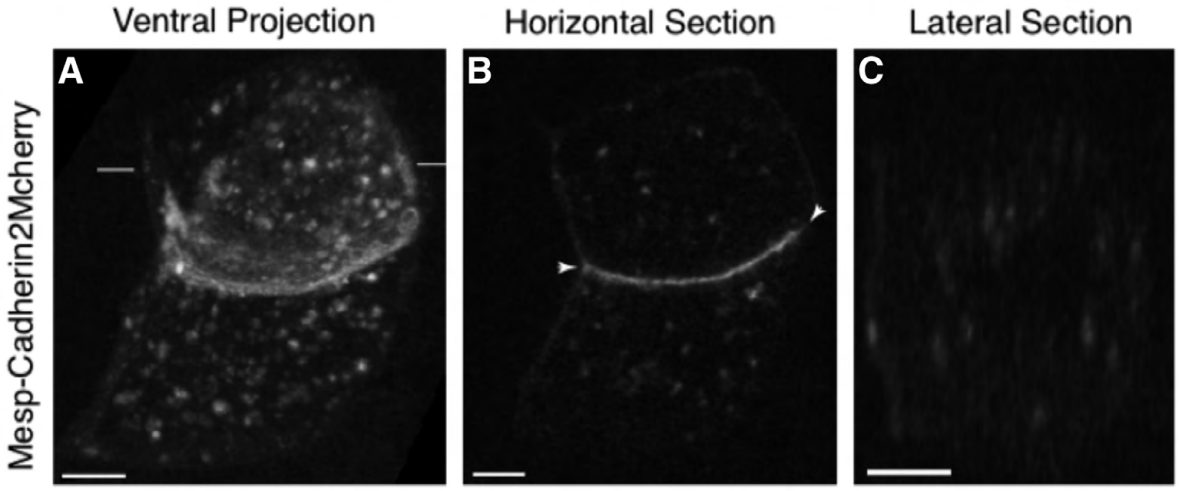

Fig. S1. Cadherin localization does not correlate with inductive signaling. (**A**) Ventral projection of representative CadherinII:3×MCherry (white)-expressing founder cells. Lines indicate approximate localization of lateral slice. (**B**,**C**) Single horizontal and lateral confocal sections; arrows indicate enrichment of cadherin fusion protein at the junction between paired founder cells. Scale bar: 5 µm. There is a lack of cadherin foci along the ventral (bottom) surface in the lateral section (C) in comparison with GFP-Talin localization (Fig. 1). CadherinI:GFP showed a similar pattern of localization (data not shown).

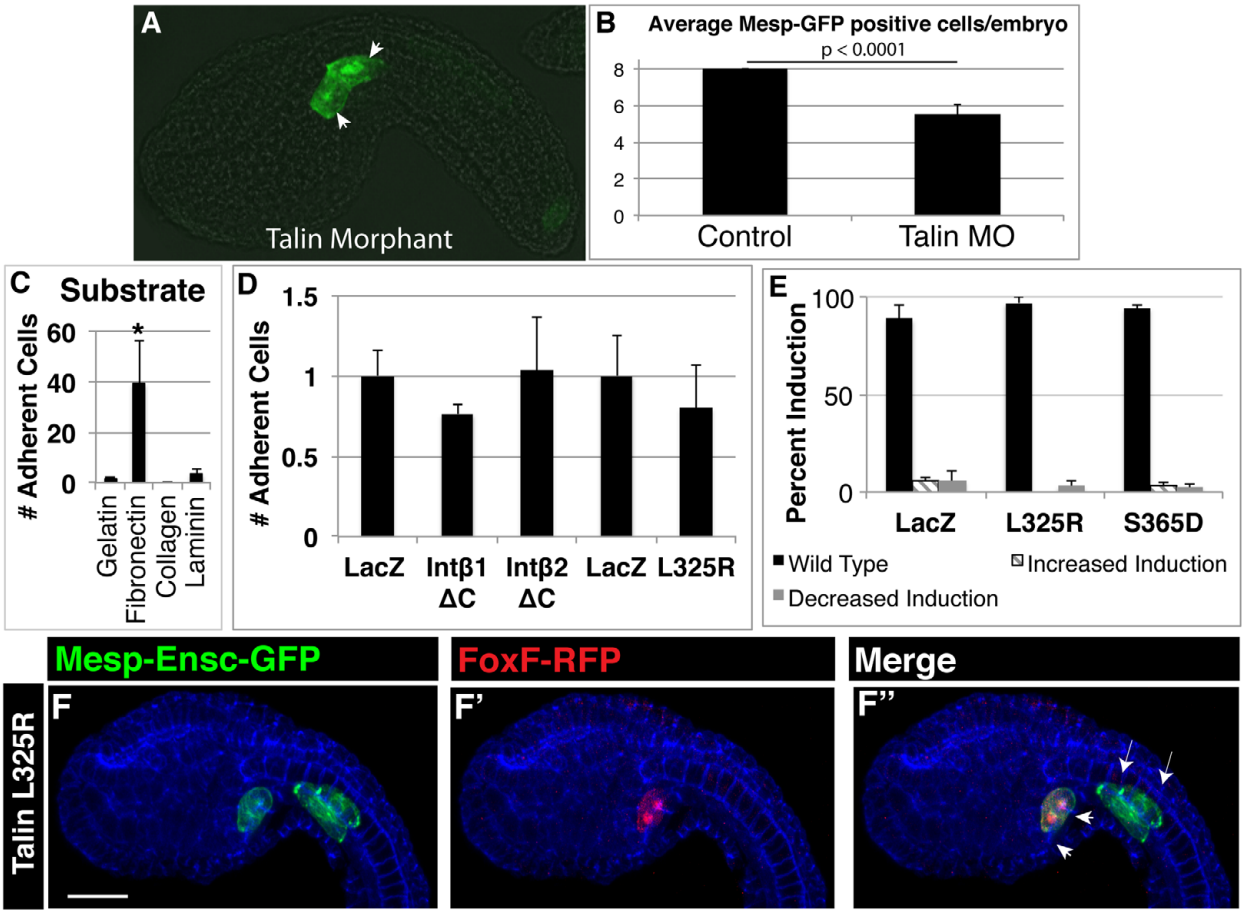

Fig. S2. Attempted disruption of integrin activation. (**A**) Lateral view of a stage 22 embyro injected with Talin morpholinos (1.0 mM/~30 pl) and Mesp-GFP displaying defective tail elongation and founder cell division. There are only two Mesp-GFP cells/side. In wild-type embryos, founder cell pairs divide asymmetrically to produce two large and two small daughters cells/side as seen in F. (**B**) Reduction of Mesp-GFP labeled founder lineage cells in Talin morphants, six trials including scoring of 53 morphants and 47 embyros injected with the 5 bp mismatch control MO. (**C**) Adhesion of dissociated transgenic founder cells to various substrates as indicated. (**D**) Talin and integrin truncation constructs show no impact on the adhesion of dissociated transgenic founder cells to fibronectin. *Ex vivo* adhesion studies were not conducted for the ΔN Integrinβ1/β2 constructs. (**E**,**F**) Graph (E) and representative micrographs (F) showing normal levels of TVC induction (FoxF-RFP) in transgenic embryos as indicated, n>42 per trial. The embryos shown in F are representative of normal TVC induction phenotypes also seen in nearly all transgenic Mesp-ΔN Integrinβ1, Mesp-ΔN Integrinβ2, Mesp-ΔC Integrinβ1 and Mesp-ΔC Integrinβ2 embryos (two trials, over 100 samples/trial). Scale bar: 20 µm.

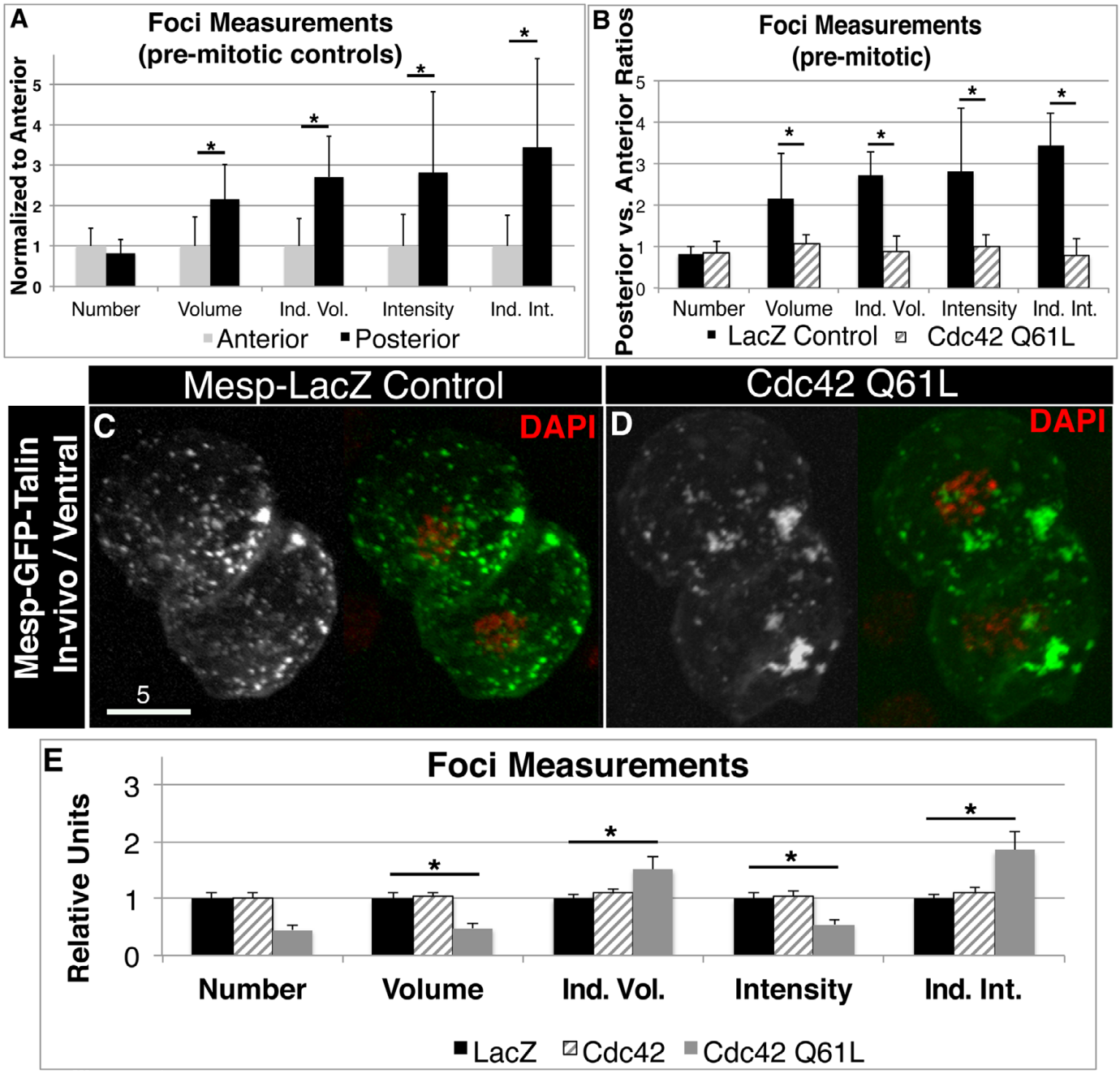

Fig. S3. CDC42QL disrupts founder cell focal adhesion dynamics. (**A**) Segmentation analysis comparing GFP-Talin foci between posterior and anterior sides of pre-mitotic transgenic Mesp-*LacZ* founder cells. **P*=0.021, 0.0074, 0.0063 and 0.00070 (left to right). (**B**) Segmentation analysis comparing pre-mitotic A/P ratios in Mesp-*LacZ* controls versus Mesp-Cdc42Q61L transgenic embryos. *P*=0.042, 0.046, 0.002 and 0.003 (left to right). For A,B, more than six founder cell pairs were analyzed for each experimental condition, each sample spanned three independent trials. (**C**,**D**) Ventral confocal projections of transgenic GFP-Talin founder cell pairs co-transfected and stained as indicated. (**E**) Segmentation analysis of GFP-Talin foci in transgenic founder cells as indicated. Asterisk indicates significant changes between *LacZ* and Cdc42Q61L focal measurements; from left to right, $P<1.25E^{-5}$, $5.87E^{-6}$, 0.04, $2.04E^{-4}$ and 0.013. More than 20 founder cell pairs for each experimental condition were examined, each sample spanned three independent trials.

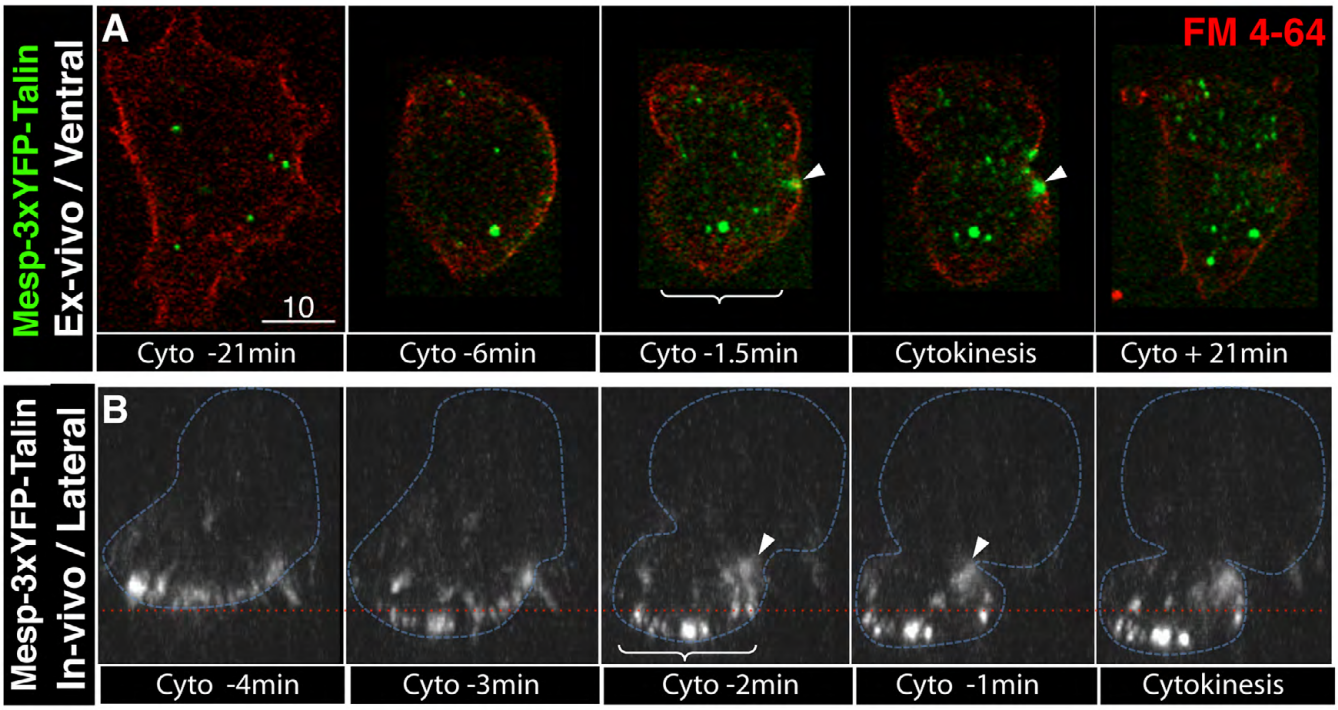

Fig. S4. Adhesive anchoring during founder cell mitosis. (**A**,**B**) Still shots from Movies S2 (A) and S4 (B) highlighting maturation of adhesive foci (YFP-Talin, green) in the dissociated founder cells (A) or in vivo (B) shortly before cytokinesis. Ventral (A) or lateral (B) confocal sections are shown. Brackets indicate initiation of regional adhesive maturation. Below each frame, time is shown relative to cytokinesis (Cyto). In A, membranes are stained with FM-464 (red). Scale for B is provided in Movie S4. YFP-Talin also accumulates in large foci along the cytokinetic ring above the plane of matrix contact, as indicated by arrows in A,B. This may reflect a role for adhesion complexes in cytokinesis as discussed previously (Pellinen et al., 2008). A role for matrix adhesion in cytokinesis might also underlie the disruption of founder cell division in Talin morphants (supplementary material Fig. S2).

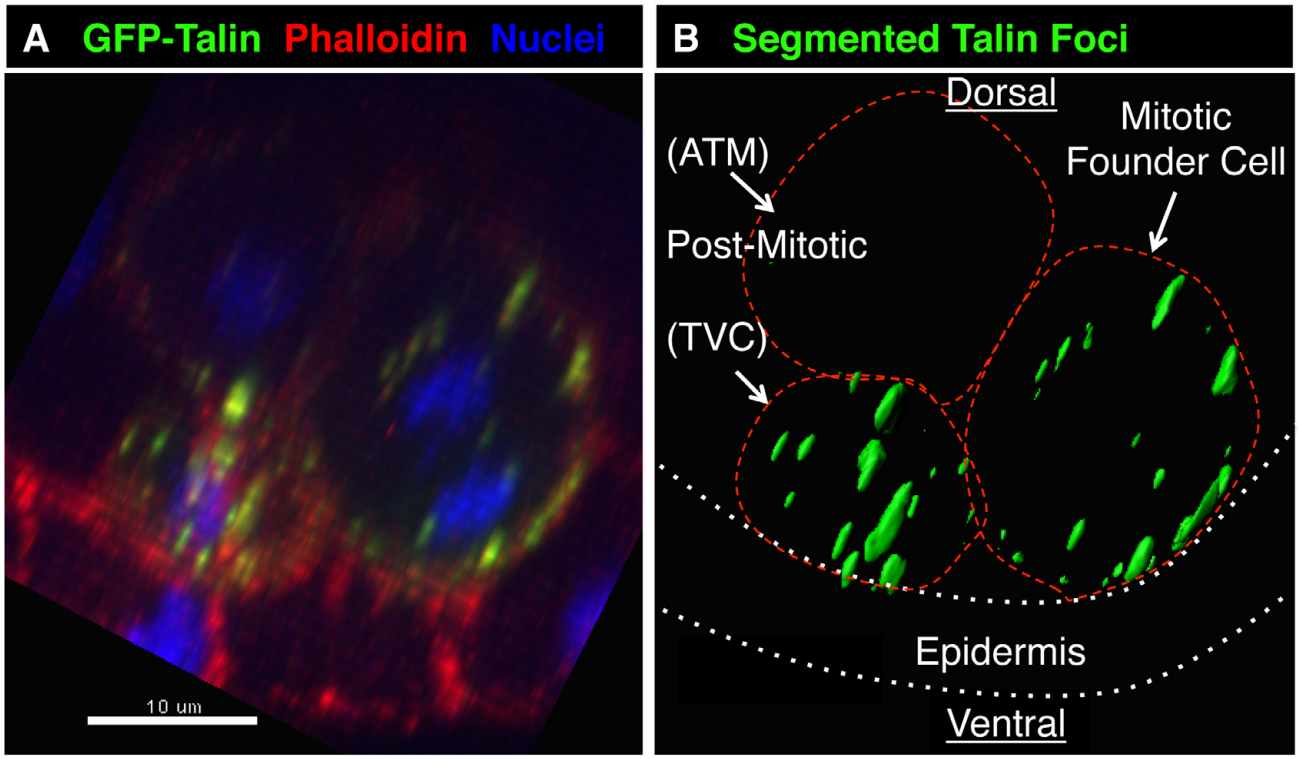

Fig. S5. Visualization and segmentation of focal adhesions. (**A**,**B**) These images provide an example of segmentation using a 5 µm projection through a pair of GFP-Talin founder cells (as labeled in B), including the raw data (A) and closely matched segmented foci (B). For characterization of GFP-Talin localization, embryos were fixed according to the *in situ* fixation protocol (Beh et al., 2007) during founder cell mitosis (6:45-6:55 hpf) and stained with antibodies against GFP (see above) along with appropriate secondaries and mounted or treated with DRAQ5 in order to determine the cell cycle stage.

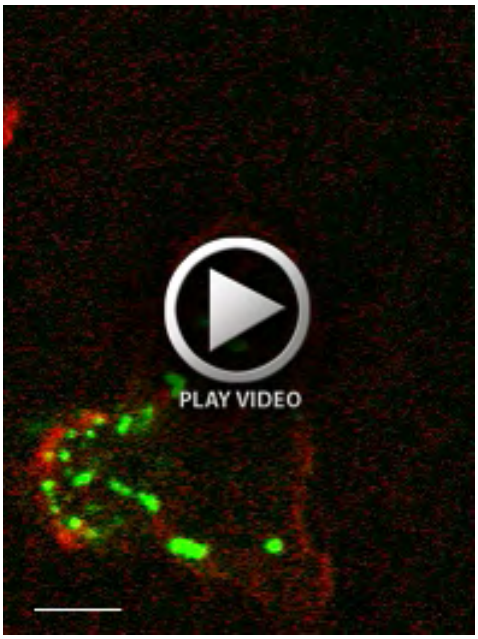

Movie 1

Movie 2

Movies 1 and 2. Dissociated GFP-Talin founder cells plated on FN and stained with FM 4-64. Red shows FM 4-64 staining. Only the ventral-most slice in contact with the FN substrate is shown. *z*-stacks were acquired every 20 seconds, 41seconds and 84 seconds for Movies 1 and 2 respectively. Scale bar: 10 μm (in Movie 1). Further information is provided in the legend for supplementary material Fig. S4.

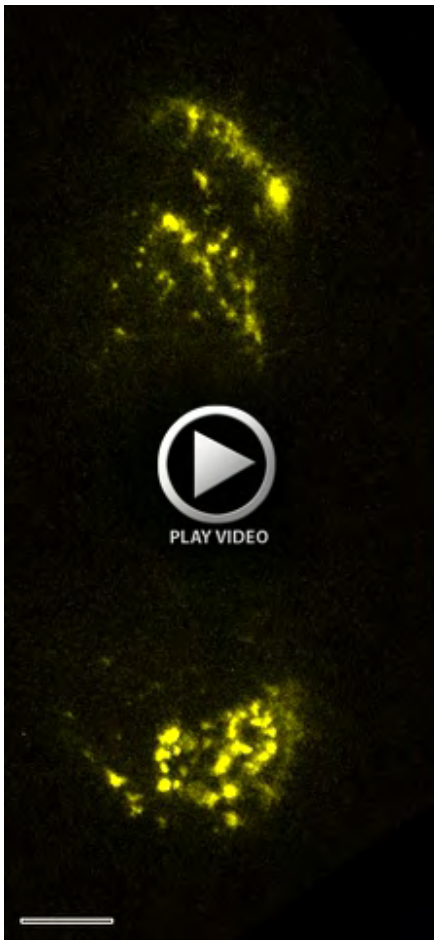

Movie 3. Ventral confocal projection of transgenic 3×YFP-Talin embryo, anterior towards the left. There are two bilateral founder cell pairs. In the top pair, which has not begun to divide at the beginning of the movie, note the initial concentration of Talin foci along posterior rim. By manually scrolling through this image sequence, it can bee seen that the bottom-most cell divides laterally, allowing a view of Talin foci maturation along the invasive membrane (arrowhead). In the medial cells, division occurs along the ventral/anterior axis. In the top medial cell, maturation of foci occurs on rounded protruding invasive membrane (arrow). *z*-stacks were acquired every 62 seconds. Scale bar: 20 μm.

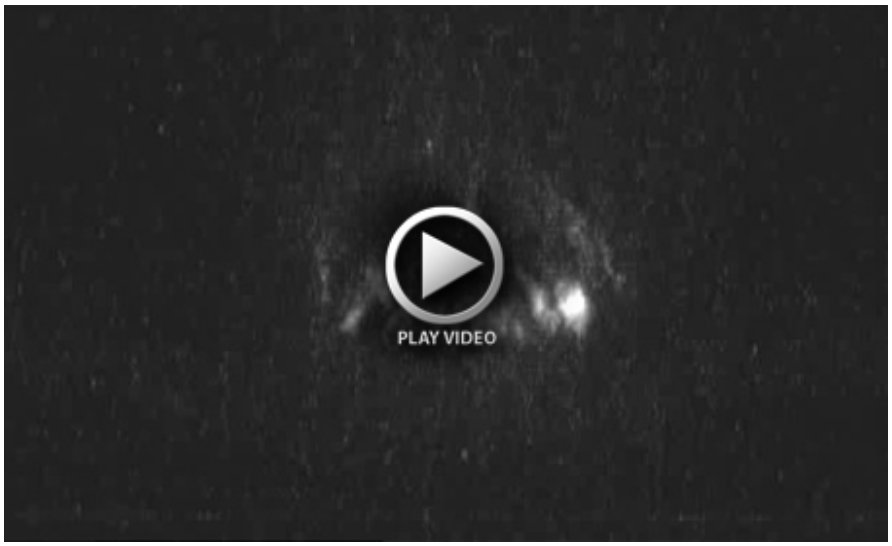

Movie 4. Lateral slice through a single founder cell from Movie 3. Anterior is towards the right (flipped in relation to panels in supplementary material Fig. S4B).

Table S1. Primers used for molecular cloning

cadhNotI5’	AAA GCGGCCGCAATAATGAGGGGAGTTGGTTCTGCAA
cadhNheI3’	AAAGCT AGCATCGCTCTCACCACCTCCGTACATAT
cadhIINotI5’	AAAGCGGCCGC CAAC ATGGAGACGATCGCTTTGCT
cadhIINheI3’	AAAGCT AGCCAGCGCTGTTTTTCGACGTCC
gfpNheI5’	AAAGCTAGCATGGTGAGCAAGGGCGAGGA
gfpEcoRI3’	AAAGAATTCTTACTTGTACAGCTCGTCCATGCCG
TalinNhe5’	aaagctagcgatttttggaagccgcaaaatcaatcgc
TalinBlp13’	aaagctcagcttaatcggattcagaatcatcc
TalinBamH15’	aaaggatccfattttggaagccgcaaaatcaatcg
3XYFP5’	aaa gcg gcc gCG CTC AAC TTT GGC AGA TCC ACC
3XYFP3’	GTAACCgGATCCGCaGCCGCATTGAAaTCAGATCTC
Intβ2Not15’	aaagcggccgtatggaaagagtaaagttg
Intβ2Blp3’	aaagctcagcgtgatgtctacgttccgtgg
IntBβΔCBlp3’	aaagctcagcggttttgtcccttcgtctacttcg
IntβGFPBamH	aaaggatccggcgttccgtggaaggttgggt
Intβ2Not15’	aaagcggccgtatggaaagagtaaagttg
Intβ2BamH13’	AAAggatccATCGGTGGTACTTTGTCCTG
Intβ2BamH15’	aaaGGATCCCTGTACCGCTAATA
Intβ2Blp3’	aaagctcagcgtgatgtctacgttccgtgg
Intβ1Not15’	gcggccgcgttattacaagcaattccaatg
Intβ1EcoR13’	aaagaATTcGTACCGTCATCACAGATTTCCAGC
Intβ1ΔC3’	aaagaattcctgctacttagggttttgagattc
Intβ1BamH15’	aaaGGATCCCGACAAAACTTGTACGACCTATGCCAATCC
Intβ1EcoR13’	aaagaATTcGTACCGTCATCACAGATTTCCAGC
Intα11Not15’	aaagcggccgccgtagtaggaatgatttactcc
Intα11Blp13’	aaagctcagcccatataagcagtgtgacagc
RapGAPNot15’	aaagcg gcc gCC ATG AAG GCT CTC CTT CGATTTCCC
RapGAPEcoR1	TTTGAAtTCATGACGTCACACC
RapNot15’	aAAGcg gCC GcT GAC AAA GGT CTA GTA ATG AGG G
RapEcoR13’	aaagaattC CGAGCTGGTTAGGGTAAGGTTAC
RapS17N	ccttggacaaattgaactgtcagtgcatttttccccacac
RapG12V	gagggaatacaagcttgttgtgcttggctctgtggg
TalinF23/F3Ec	aaagaattcttattttagaataatgtcaatgtatccagc
TalinF3Not15’	aaagcggccgccggggtcacatttttcttagttaagg
TalinF23Not15’	aaagcggccgccaagtatttttattcagatcaaaacgttg
L335R	tgaaaggccgaaacaagcgggttccacgtttgatgggagtc
S365D	gatgggctgcttcaccaaaagatttcactctggactttgg
PaxGFPNot15’	Aaa gcg gcc
PaxBamH13’	aaaGGgaTcCCCAACATTAGGAAGGCCATAAAGC

All Mesp-Cadherin fusion constructs were built by Katerina Ragkousi (University of Arizona) as follows. The *cadherin* gene was amplified from the vector VES91_B10 (Cogenics) with cadhNotI5’and cadhNheI3’. The *cadherin II* gene was amplified from the vector VES104_F13 (Cogenics) with cadhIINotI5’ and cadhIINheI3’. The *gfp* and *cherry* genes were amplified from vectors Ttf-GFP-Strabismus (Ragkousi et al., 2011) and pRN3-Nter-mCherry (Hitoyoshi Yasuo, UPMC-CNRS), respectively, with:gfpNheI5’ and gfpEcoRI3’. The amplified *gfp*-, *cherry*- and cadherin-coding regions were cloned into *Nhe*I-*Eco*RI and *Not*I-*Nhe*I of the Mesp-GFP-Strabismus vector (Ragkousi et al., 2011). The TalinA C-terminal fragment in GFP-Talin and 3×YFP-Talin was amplified from the *Ciona intestinalis* Gene Collection Release 1 (Satou et al., 2002) clone id # GC25k21 and cloned downstream of the Mesp enhancer

using TalinFNhe5′ and TalinBlp13′. The Talin A fragment was then re-amplified from the above plasmid and cloned downstream of Mesp-3×YFP using TalinBamH15′ and TalinBlp13′. Mesp-3xYFP was built using a 3×YFP construct generously provided by Hitoyoshi Yasuo (UPMC-CNRS) cloned downstream of the Mesp enhancer using 3×YFP5′ and 3×YFP3′. The Integrin β2 fragment in Mesp-Integrinβ2, was amplified from the full open reading frame unigene collection clone ID# VES70_P04 (Cogenics) and cloned downstream of the Mesp enhancer using the following primers: Intβ2Not15′ and Intβ2Blp3′. The Mesp-Integrinβ2ΔC truncation and Mesp-Integrinβ2-GFP were made using the Mesp-Integrinβ2 plasmid described above with the following primers: IntBβΔCBlp3′ and IntβGFPBamH13′. The Mesp-Integrinβ2ΔN mutant was constructed from two fragments: (1) the predicted signal sequence of Integrin B2 (SignalIP, http://www.cbs.dtu.dk/services/SignalP/) amplified using the primers Intβ2Not15′ and Intβ2BamH13′; and (2) The C-terminal transmembrane and intracellular domain of Integrin β2 using primers Intβ2BamH15′ and Intβ2Blp3′. The Integrin β1 fragment in Mesp-Integrinβ1, was amplified from the full open reading frame unigene collection clone ID# VES64_B11 (Cogenics) and cloned downstream of the Mesp enhancer using: Intβ1Not15′ and Intβ1EcoR13′. The Mesp-Integrinβ1ΔC truncation was made by amplfying the plasmid described above with Intβ1ΔC3′. The Mesp-Integrinβ1ΔN truncation was made by amplifying the C-terminal intracellular region of Integrinβ1 from the above plasmid and inserting it after the signal sequence of the Mesp-Integrinβ2ΔN plasmid described above using Intβ1BamH15′ and Intβ1EcoR13′. The Integrin α11 fragment in Mesp-Integrinα11 was amplified from the full open reading frame unigene collection clone ID# VES95_N23 (Cogenics) and cloned downstream of the Mesp enhancer using Intα11Not15′ and Intα11Blp13′. The Intα11-GFP was amplified from the plasmid described above using Intα11Not15′ and IntGFPBamH13′. The RapGAP fragment was amplified from the full open reading frame unigene collection clone ID# VES7k09 (Cogenics) and cloned downstream of the Mesp enhancer using RapGAPNot15′ and RapGAPEcoR13′. Full-length Rap was amplified from ID# VES79p15 (Cogenics) and cloned downstream of the Mesp enhancer using RapNot15′ and RapBamH13′. The mutations in Mesp-RapS17N and Mesp-RapG12V were made using site-directed mutagenesis of the Mesp–Rap plasmid described above with forward a reverse RapS17N or RapG12V primers. The coding sequences used for the Talin F23 and F3 fragments in Mesp-TalinF23, Mesp-TalinF3L325R and Mesp-TalinF3S365D were amplified from cDNA libraries made from total RNA using Trizol LS reagent (Invitrogen #10296-028) according to the manufacturer's protocol, and cDNA was prepared using the M-MLV reverse-transcriptase system (Invitrogen # 28025-01). Fragments were amplified for insertion downstream of the Mesp enhancer using: TalinF23/F3Eco3′, TalinF3Not15′ and TalinF23Not15′. The Mesp-TalinF3 mutations were made using site-directed mutagenesis of the Mesp-TalinF3 plasmid described above with forward and reverse L335R and S365D primers. The Paxillin fragment in Paxillin-GFP was amplified from the from the full open reading frame unigene collection clone ID# VES57D12 (Cogenics) and cloned downstream of the Mesp enhancer using: PaxGFPNot15′ and PaxBamH13′.

Table S2. Cell counts for *ex vivo* adhesion assays

Fig. 2A	(*LacZ* control=49±17::5.15±0.31 versus RapS17N=1.0±1.7::4.86±2.38, *LacZ* control=130±5.1::5.29±0.95 versus RapGAP=4.3±2.5::4.79±2.31).
Fig. 3A	(*LacZ* control = same as Fig. 1A RapS17N control versus RapG12V=75±33::5.01±1.69, *LacZ* control=163±82::1.92±1.33 versus TalinF23=115±89::1.94±1.94).
Fig. 4A	(RapS17N control = same sample set as in Fig. 1A versus RapS17N+Intß1=0.67±1.1::4.89±2.38×10^5 or RapS17N+Intβ2=7.0±3.6::4.47±2.40×10^5 , RapDN control=5.3±2.5::1.30±1.01×10^5 versus RapS17N+IntA11=5.3±6.7::1.13±0.76×10^5).
Fig. 6I	(*LacZ* control=221±73::3.63±0.23×10^5 versus CDC42Q61L=73±9.4::2.87±2.72×10^5, RapS17N control=5.3±0.85::4.34±2.98x10^5 versus RapS17N+CDC42Q61L=6.1±0.91::4.38±2.58×10^5).
Fig. S2	(*LacZ* control=92±26::1.11±0.40×10^5 versus Intß1ΔC=65±48::1.35±1.60×10^5 or Intß2ΔC=60±23::1.25±1.45×10^5, *LacZ* control = same as Fig. 3A TalinF23 control versus TalinL325R=84±87::1.45±1.83×10^5).

Raw average values ±s.d. for each of the sample sets (adherent cells::estimated cell density ×10^5).